Applied Science and Engineering Progress, Vol. 13, No. 1, pp. 48–55, 2020

Research Article

Materials Characterization Techniques for the Analyses of Components of Port Fuel Injectors

Joe Yenube Lambongang* and Piyada Suwanpinij
The Sirindhorn International Thai-German Graduate School of Engineering (TGGS), King Mongkut's University of Technology North Bangkok, Bangkok, Thailand

* Corresponding author. E-mail: joeyenube@gmail.com DOI: 10.14416/j.ijast.2018.11.008
Received: 24 February 2018; Revised: 23 March 2018; Accepted: 11 May 2018; Published online: 27 November 2018

Abstract
Recent materials for port fuel injector components undergo diverse feature changing manufacturing processes. These extra features enable them to withstand the harsh environments they are subject to. This makes the analyses of such small port fuel injector materials a daunting task after their manufacture. This study analyzes various characterization techniques of different probe sizes and atmospheric conditions. It determines the ideal techniques to use when analyzing materials of different types of port fuel injectors after their manufacture. In quantitative chemical analysis, the presence of monochromator and vacuum, produced reliable results in the case of X-ray Fluorescent Spectroscopy (XRF) with X-ray tube. Fabrication techniques and the stainless steel groups of the components were also found to influence which techniques work best.

Keywords: Materials, Characterization, Injector, Components

1 Introduction

The importance of material characterization cannot be over emphasized. In an ideal world an extrinsic property of a material is a function of its intrinsic characteristics [1]. This makes the analysis of material properties very necessary in making a well-informed conclusion regarding factors such as functional abilities. However, looking for the right materials characterization techniques to determine differences existing between small and complicated engine parts could be a daunting task. Most materials characterization techniques are ideal for bigger samples. It is also more complicated when the samples in question have undergone several feature changing processes. These processes enable them to possess extra features such as; the ability to withstand harsh conditions like high temperature, high pressure and corrosive environment [2], [3]. The extra features acquired mostly have an influence on the results of some characterization techniques that rely on properties such as hardness and magnetic properties of the samples. This makes it imperative to conduct further experiments with other techniques and atmospheric conditions before more reliable results could be achieved.

In this study, analyses of several materials characterization techniques were made with different samples. The study determines the ideal techniques and conditions to use for samples from complicated components such as port fuel injectors. It is particularly necessary when an improvement on the functional abilities is desired by a different manufacturer who has no knowledge of the original state of materials due to confidentiality issues.

Port fuel injectors are small engine components that supply fuel to the intake manifold of the engines of automobiles [2], [3]. They are made to withstand harsh operating conditions [4]. The operating conditions

Please cite this article as: J. Y. Lambongang and P. Suwanpinij, "Materials characterization techniques for the analyses of components of port fuel injectors," *Applied Science and Engineering Progress*, vol. 13, no. 1, pp. 48–55, Jan.–Mar. 2020.

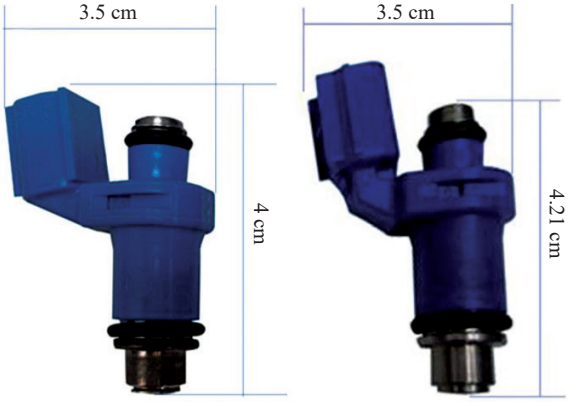

Figure 1: Port fuel injectors of type 1 (right) and type 2 (left) after their manufacture.

include an ambient temperature of –40°C to +140°C, fuel temperature at inlet from –40°C to +70°C, manifold pressure of ≤ 250 kPa etc. Their components go through diverse manufacturing processes to possess this ability. Several properties including hardness are greatly influenced by fabrication techniques such as deep drawing, forging etc. Such properties are required for effective functioning.

Port fuel injectors of two different types were studied to determine their original materials and the differences existing between them. One injector uses ethanol as fuel (indicated as type 1). The other cannot use ethanol as fuel (indicated as type 2). Each injector is composed of 12 metallic components and 5 polymer components. The lengths of the components vary from as tiny as 1 mm, to a maximum length of 18.62 mm.

Materials characterization techniques come in either destructive or nondestructive form. Nondestructive techniques were employed first before destructive techniques to minimize wastage of samples. Disassembly of both injectors was imperative in order access all the components. It was done after observing the nature of the inner components with the help of industrial CT scan.

The observation of the inner components with industrial CT scan made it possible to locate the delicate components such as the terminal clip in order not to mistakenly destroy them during disassembly. It also gave an idea concerning the number of components to expect from each injector after disassembly.

Figure 1 shows the appearance of both injectors before disassembly. Figure 2 shows the inner parts of the injectors captured by industrial CT scan.

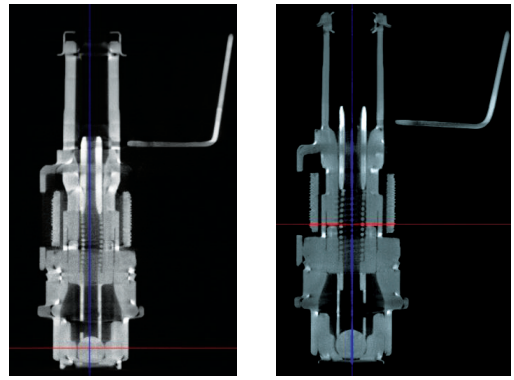

Figure 2: CT scan revealing the inner components of both types of port fuel injectors (type 1 (left) and type 2 (right)).

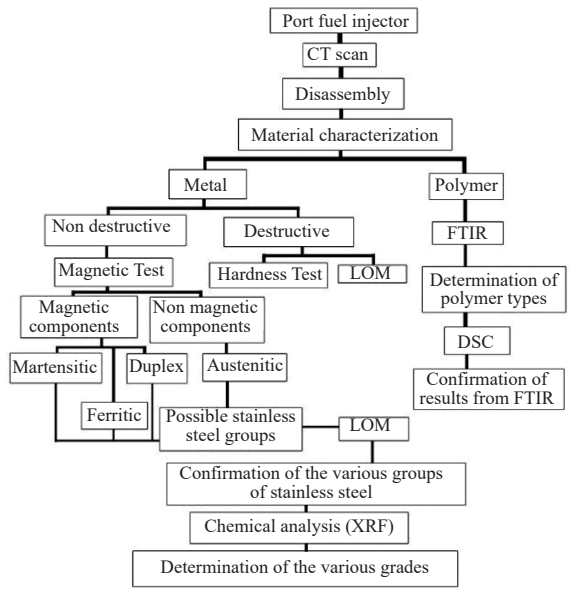

Figure 3: A diagrammatic description of the entire workflow.

2 Experimental Procedure

Figure 3 shows a description of the entire workflow.

2.1 *Disassembly of the injector*

The disassembly was performed after industrial CT scan had revealed all the components of the injectors. Due to the sizes of the injectors, a bench vise was used to hold the workpiece firmly before certain

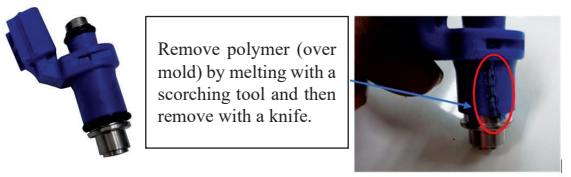

Figure 4: Polymer being removed by melting with a heated scorching tool.

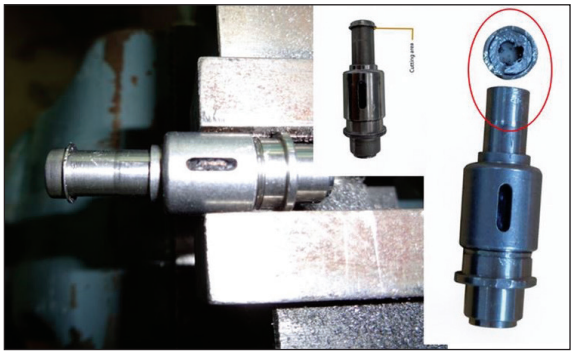

Figure 5: Fully clamped injector, while its filter is being cut off.

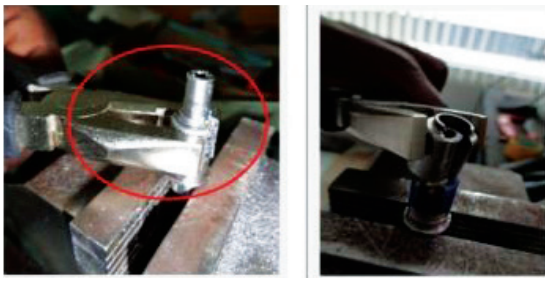

Figure 6: Shell being removed by turning from left to right and then upwards with a pair of pliers.

components could be cut off. The polymer was removed using a heated scorching tool to slightly burn, followed by removal using a cutting knife. Different sizes of spanners and pliers were also used to remove the tightly fixed parts. Figures 4–10 explain the entire disassembly process.

2.2 *Materials testing for materials properties for narrowing down the possible materials grades*

Differentiation of samples belonging to ferritic, austenitic, martensitic and duplex stainless steel was made possible using a small neodymium magnet; not

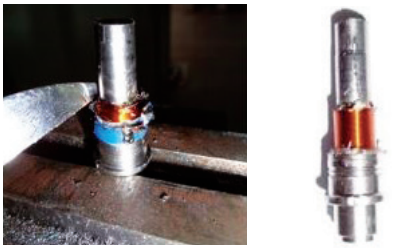

Figure 7: Polymer being removed with a cutting knife after it has been melted.

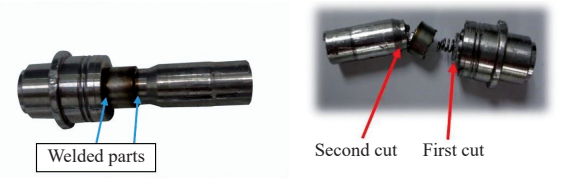

Figure 8: Welded parts being cut to expose and remove inner components.

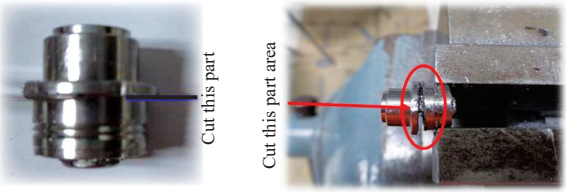

Figure 9: Seat carrier being cut to expose the valve seat.

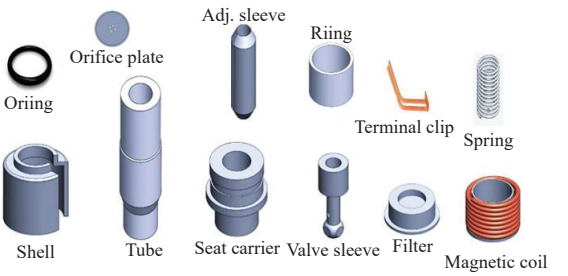

Figure 10: Components of the port fuel injector without polymer case (overmold).

forgetting the fact that deformation could cause a massive change in the magnetic properties of austenitic grades. To minimize waste, XRF and Light Optical Microscopy (LOM) were performed before hardness testing according to American Society for Testing and Materials (ASTM) standard E92-82. The hardness values of the samples also gave an idea about the possible groups of stainless steel.

2.3 *Microstructure analysis*

The microstructure of the matrix was investigated using LOM to group the metals into the various groups of stainless steel (i.e., ferritic, martensitic, austenitic and duplex stainless steel). LOM was done since knowledge of the microstructure of every sample was highly essential in determining the possible stainless steel groups that they could belong to. Cold mounting, grinding and polishing of the samples according to International Organization for standardization (ISO) standards were done. The various etchants included:

- Nital (122 mL C_2H_5O (alcohol) + 122 mL HCl (hydrochloric acid) + 6 mL HNO3 Nitric acid),
- Ralph's reagent (100 cc H_2O +200 cc methyl alcohol + 100 cc HCL + 2g $CuCl_2$ + 7g $FeCl_2$ + 5 cc HNO3),
- Viella's reagent (5 cc HCl + 2g Picric acid + 100 cc Ethyl alcohol),
- Glyceregia (15 cc HCl + 10 cc Glycerol + 5cc HNO_3 (standard concentration),
- Color etchant (100 mL of stock solution +1g of potassium bisulphite).

2.4 *Chemical analysis*

In chemical analysis, both XRF with standard probe (with a detector of 18 mm diameter by 44 mm long) and μXRF were considered. However, due to the small and interconnected nature of the components; μXRF was preferred.

XRF spectrometer, Rh 4 kW (ZSX Primus, Rigaku, Japan); which uses X-ray tube was used. It has a beam size of 0.5–30 mm and with WDS vacuum. The diaphragm was adjusted for the various components within a range of 0.5–10 mm.

2.5 *Polymer analysis*

Fourier Transform InfraRed spectroscopy (FTIR) was used for the determination of the polymer types. Differential Scanning Calorimeter (DSC) was employed for the separation of the polymer components.

The FTIR experiment was achieved using a spectrometer model called Nicolet 6700, Thermo-Scientific, USA, together with OMNIC software. The number of scans were 64 times at a resolution of 4 cm^{-1}.

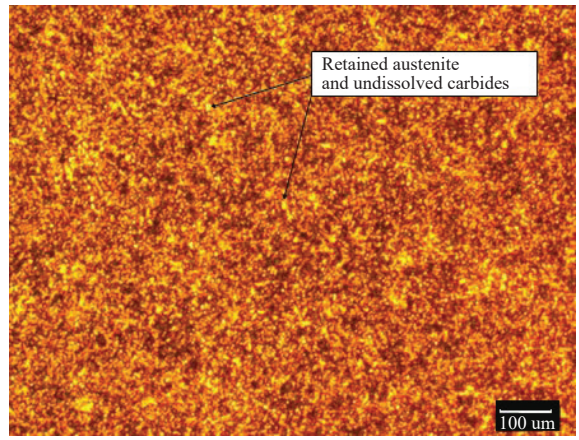

Figure 11: Microstructure of a type 2 component etched with Viella's reagent, captured under 200X magnification and has a hardness value of 699.2 HV1.

Mettler Toledo TGA/DSC 3+ was used for the DSC experiment with a starting temperature of 30 and 650°C as ending temperature and a scan rate of 10°C.

3 Results and Discussion

3.1 *Results and discussions of LOM and hardness tests*

LOM analysis with various etchants were used until the most appropriate ones could be determined. Glyceregia, Viella's reagent and color etchant were discovered to be the most ideal etchants depending on the stainless steel groups that the injectors' components belong to.

Figures 12 and 13 show different stainless steel groups etched with glyceregia and most of the vital information needed to determine their groups is made available. Viella's reagent was ideal for martensitic components but not ideal for components belonging to other groups. This is because after numerous experiments with Viella's reagent, the microstructures of samples from the injectors' components belonging to other groups of stainless steel could still not be revealed. A few grain boundaries were revealed. However, not enough for a firm conclusion to be made regarding the stainless steel groups of the samples.

Figure 11 shows the microstructure of a type 2 component. It was etched with Viella's reagent after magnetic tests showed that it is magnetic. It shows the extent to which the etchant has revealed its features needed to determine the stainless steel group to which

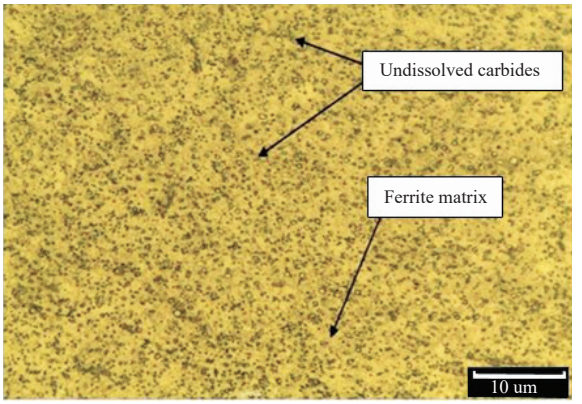

Figure 12: Microstructure of a type 2 component etched with glyceregia, captured under 500X magnification and has a hardness of 696 HV0.5.

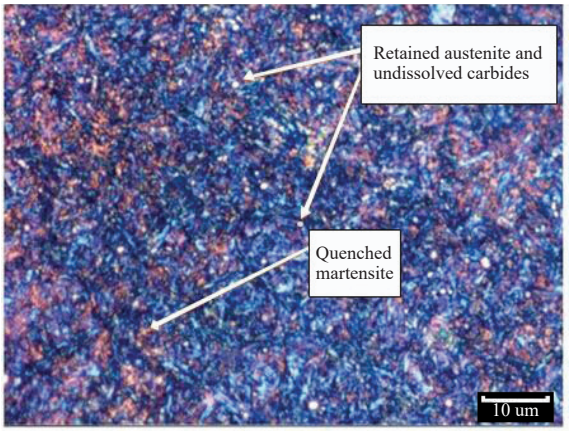

Figure 14: Result of color etching of a type 1 component captured under 500X magnification.

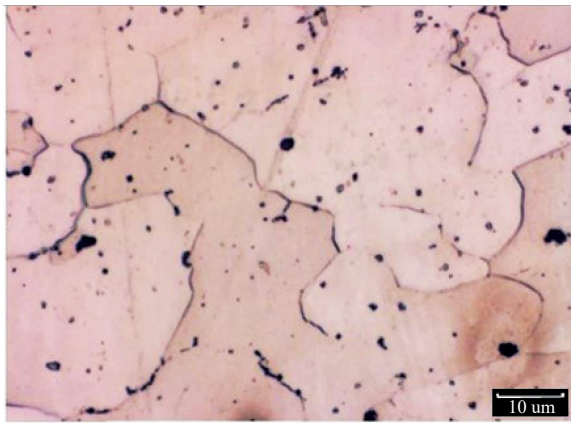

Figure 13: Microstructure of a type 1 component etched with glyceregia, captured under 500X magnification and has a hardness of 228 HV1.

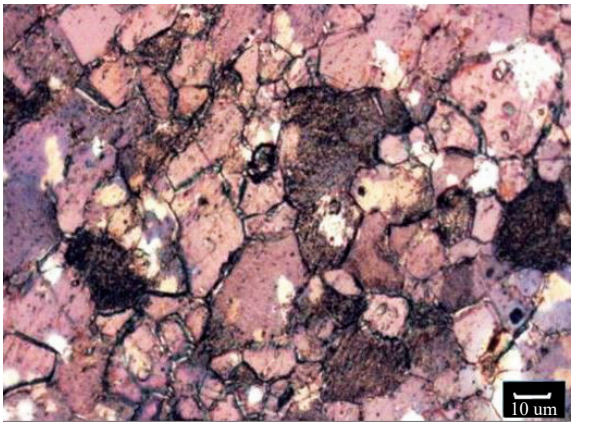

Figure 15: Ferritic microstructure by color etching captured under 200X magnification.

it belongs. The revelation of features such as retained austenite and undissolved carbide indicate that it is made of martensitic stainless steel [5].

Figure 12 shows the microstructure of a component etched with glyceregia. Traces of undissolved carbides are observed to be deposited in the sample's matrix indicating that the sample is made of martensitic stainless steel [5].

The microstructure of a component etched with glyceregia is shown in Figure 13. This component is magnetic. The microstructure is devoid of undissolved carbides, quenched martensite, twinning, and does not have a dual phase. This gives a high indication that the sample could be made of ferritic stainless steel. This was substantiated during chemical analysis by μXRF.

Color etching in Figure 14 reveals vital features such as retained austenite, undissolved carbide and quenched maternsite. Such features are needed in determining the stainless steel group of the sample. Figure 14 component is magnetic and shows the presence of retained austenite, undissolved carbides and quenched martensite. These features are synonymous with martensitic stainless steel [5].

In Figure 15, color etching has revealed the properties of the sample's microstructure. This sample is the same as that of Figure 13. Color etching in this case has also etched the sample to show important features. However, when compared with Figure 13 which was etched with glyceregia, the details of color

etching is not as clear as that of glyceregia. Though it still reveals enough properties to determine its stainless steel group.

Micro Vickers hardness test gave relevant information regarding stainless steel groups. The results were compared with that of techiques such as LOM and μXRF before a reliable conclusion was made regarding the stainless steel groups and grades. For instance, the hardness value of a type 1 component (tube) made by deep drawing method was 342 HV0.5. This gave the indication that it could belong to martensitic group [6], [7]. However, microstructure analysis and chemical analysis suggested it was a ferritic stainless steel (AISI 405) and was supposed to have a hardness of about 190 HV0.5.

3.2 *Results and discussions of XRF experiment*

Table 1 shows the μXRF results of a type 1 component. This was the same sample used for Figure 13. Microstructure analysis from Figure 13 indicated that the sample is of ferritic stainless steel. Table 1 shows a comparison between the elements present in the sample and that of stainless steel AISI 405. The results indicate that the sample corresponds to stainless steel AISI 405 [6]–[8].

Table 1: Results from μXRF experiment of a type 1 component, showing the composition of all elements present

Elements Present	Quantitative Results of Elements (%)	Standard (AISI 405) [5]
Cr	13.4746	11.50–14.50
Al	0.2911	0.10–0.30
Si	0.7778	Max 1.00
Mn	0.2113	Max 1.00
Fe	82.0049	~85
Ni	0.2267	-
Mo	0.1231	-
Cu	0.0789	-
Pb	0.1257	-

Information concerning the chemical composition of a type 2 component is shown in Table 2. The composition of each element was compared with that of stainless steel AISI 405. The results indicate this component corresponds to stainless steel AISI 405 [6]–[8].

Table 2 : Results from μXRF experiment of a type 2 component, showing the composition of all elements present

Elements Present	Quantitative Results of Elements (%)	Standard (AISI 405) [5]
Cr	13.5929	11.50–14.50
Al	0.2934	0.10–0.30
Si	0.8941	Max 1.00
Mn	0.2013	Max 1.00
Fe	80.6277	~85
Ni	0.2945	-
Mo	0.1558	-
Cu	0.1183	-

μXRF with X-ray tube and beam size of 0.5–30 mm with WDS vacuum, proved to be more ideal for quantitative analysis. This is because μXRF with X-ray tube selects single wavelength because of the presence of monochromator.

Secondly, μXRF with X-ray tube has vacuum and can measure light elements. Hence, these factors make μXRF with X-ray tube more accurate and reliable for quantitative analysis of metallic components of port fuel injectors.

3.3 *Results and discussions of polymer*

The FTIR result in Figure 16 gives information concerning the wavelength and absorbance of the polymer case (overmold).

The result shows high peaks at different wavenumbers. Observations from left to right show the first peak at 3299.62 wavelength. This peak fall specifically under alcohol O-H group [9], [10]. The next two peaks are exactly on the 2926.68 and 2856.19 respectively, which also belong to sp3 C-H group [9], [10]. All peaks ranging between 1000 and 1350 are either C-C, C-N or C-O single or double bonds [9], [10]. The peaks that fall between 1600 and 2260 wavelength represent C=C (double bond), C=N (double bond), C=O (double bond), C ≡ O (triple bond) or C ≡ N (triple bond) [9], [10].

Figure 17 shows the nature of the wavelength closely corresponds to several polymer types including polyamide 6, polyamide 66, polyamide 6 + polyamide 66 etc.

In DSC experiment of the same sample, a melting temperature of 246.36°C was recorded. When compared

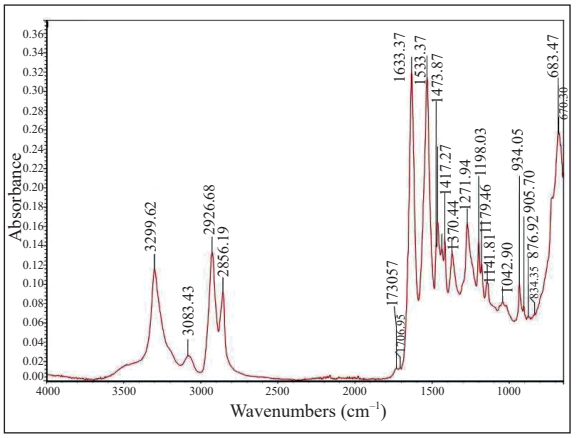

Figure 16: FTIR result of polymer case (overmold), showing the wavenumbers and absorbance of all peaks.

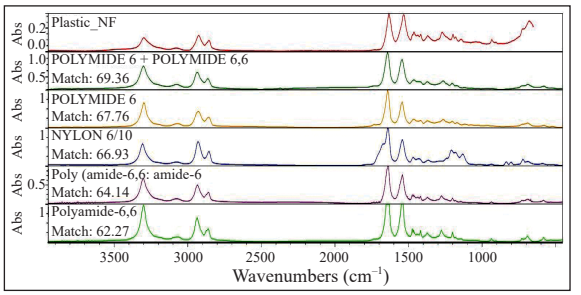

Figure 17: FTIR results of polymer case (overmold) being compared with other types.

with the melting temperatures of all the polymer types in Figure 17, it falls in between polyamide 6 and polyamide 66 which have melting temperatures of 210–220°C and 255–268°C respectively [11], [12]. This gives an indication that the material could most likely be made of a combination of polyamide 6 and polyamide 66 (i.e., PA 6+PA 66). This is because the melting temperature of the sample does not completely fall within a specific type but rather falls in between the two types.

This means the result from DSC conforms to the FTIR result in Figure 17 which shows a wavelength that corresponds to a number of types including polyamide 6+polyamide 66 which has the closest match.

4 Conclusions

The stainless steel groups of components such as the seat carrier, filter etc. were determined by Vickers hardness test. In some cases where the stainless steel groups were still doubtful due to a suspicion of influence from fabrication techniques, microstructure analysis and chemical analysis were performed to support those results from hardness test.

Therefore, in analyzing materials of such nature, hardness test must always be accompanied with microstructure analysis and chemical analysis for confirmation.

LOM analysis using different etchants have been performed. It can therefore be concluded that when vital microstructure information such as grain boundaries, twinning, quenched martensite, etc. of unknown materials of such nature are sought after, it is more ideal to use glyceregia or color etchant. This is because they both work well for all stainless steel groups irrespective of the kind of fabrication processes that the samples might have been through.

Viella's reagent on the other hand proved to be mostly ideal for martensitic components. In the case of other stainless steel groups, Viella's reagent could not reveal the features of the microstructure clearly as in the case of glyceregia and color etchant.

In quantitative chemical analysis, μXRF with X-ray tube has proven to be more reliable in giving accurate results for metallic components of port fuel injectors. This is because of the presence of monochromator and vacuum. This factor makes it possible for single wavelength to be selected and allows the analyses of all elements including light elements.

LOM, μXRF, magnetic and hardness experiments revealed that type 1 needle valve is made of AISI 405 (ferritic), while type 2 needle valve is made of AISI 302 (austenitic).

CT scan and microscopic view of the balls of both types revealed that type 1 ball has both flattened and rounded surfaces, while type 2 ball has only rounded surface.

A cross sectional cut and a microscopic view of both types of valve seat revealed a difference in their designs. This difference is believed to have been made to accommodate the designs and dimensions of the balls found in both types of port fuel injectors.

Acknowledgement

The authors would like to express profound gratitude to Associate Professor Siriporn Daopiset and Assistant

Professor Dr. Peerawatt Nunthavarawong for their support.

References

[1] J. W. McCauley and V. Weiss, "Materials characterization for systems performance and reliability," in *Proceedings Sagamore Army Materials Research Conference Proceedings 31*, 1986, p. 2.

[2] A. Wade, *Motorcycle Fuel Injection Handbook*, 2nd ed., Wisconsin: Motorbooks International, 2004, p. 47.

[3] N. Enright, "Basic principles of operation and applications of fuel injection systems in petrol powered cars," Department of Mechanical & Automobile Engineering, Limerick Institute of Technology, Limerick, Ireland, 2015.

[4] R. M. Campion, C. Q. Dam, K. W. Hall, and W. J. Rodier, "Coatings for use in fuel injection components" U.S. Patent 7942343B2, Sep. 21 1998.

[5] L. B. Ramos, "Tribocorrosion and electrochemical behaviour of din 1.4110 martensitic stainless steels after cryogenic heat treatment," *Materials Research*, vol. 20, pp. 2, Feb. 2017.

[6] G. V. Voort, *ASM Handbook Volume 9: Metallography and Microstructures*. Ohio: ASM International, 2004, pp. 675–699.

[7] *Stainless Steel Database*, Atlas Steel Co., Ohio, USA, 2013, pp. 2–57.

[8] *Handbook of Stainless Steel*, Stainless steel categories and grades, Helsinki, Finland, 2013, pp. 10–20.

[9] B. Stuart, *Infrared Spectroscopy: Fundamentals and Applications*. Chichester: John Wiley and Sons Ltd, 2004.

[10] N. Cheval, N. Gindy, C. Flowkes, and A. Fahmi, "Polyamide 66 microspheres metallised with in situ synthesized gold nanoparticles for a catalytic application," *Nanoscale Research Letters*, vol. 7, no. 1, p. 182, Mar. 2012.

[11] T. R. Crompton, *Fourier Induced Transform Spectroscopy*. UK: Lightning Source Ltd, 2006, pp. 85–86.

[12] A. R. Bunsell, *Handbook of Tensile Properties of Textile and Technical Fibres*, 2nd ed., Cambridge, UK: Woodhead Publishing, 2018, pp. 200–219.